Tumor targeted and GSH stimuli-response α#lactalbumin nanotubes co-delivering doxorubicin and siRNA for cancer therapy

Author(s):
Hou, Guohua; Wu, Di; Li, Xing; Liu, Bin

Publication date:
2024-12

Permanent link:
https://doi.org/10.3929/ethz-b-000651413

Originally published in:
Journal of Future Foods 4(4), https://doi.org/10.1016/j.jfutfo.2023.11.002

Available online at www.sciencedirect.com

Journal of Future Foods

Journal of Future Foods 4-4 (2024) 300–308

journal homepage: http://www.keaipublishing.com/en/journals/journal-of-future-foods

Tumor targeted and GSH stimuli-response α-lactalbumin nanotubes co-delivering doxorubicin and siRNA for cancer therapy

Guohua Hou[a], Di Wu[c], Xing Li[a,*], Bin Liu[a,b,*]

[a] Research Center of Food Colloids and Delivery of Functionality, College of Food Science and Nutritional Engineering, China Agricultural University, Beijing 100083, China
[b] Department of Nutrition and Health, China Agricultural University, Beijing 100193, China
[c] Department of Health Sciences and Technology, Eidgenössische Technische Hochschule Zürich, Zürich 8092, Switzerland

ARTICLE INFO

Article history:
Received 24 October 2022
Received in revised form 9 January 2023
Accepted 5 February 2023
Available Online 30 November 2023

Keywords:
α-Lactalbumin nanotube
Nanocarrier
Tumor-targeted
siRNA
Synergistic effect

ABSTRACT

α-Lactalbumin (α-lac), a natural food-sourced protein, exhibits high biocompatibility as delivery systems for small bioactive molecules or RNA. However, their potential clinical application as a delivery system is greatly limited due to the lack of targeting to desired tissues, such as tumors. Here, a delivery system/nanocarrier of nanotube (NT) was fabricated by the self-assembly of peptides hydrolyzed from α-lac. Among the loading of anti-tumor agents of doxorubicin (Dox) and siRNA, NTs were conjugated with the tLyp-1 peptide to specifically target the neuropilin 1 receptor, which exists on the membrane of MDA-MB-231 cancer cells. The micromorphology of NTs was not affected during the processes of loading and targeting modification. Additionally, no significant changes in the size and zeta potential of the tLyp-1/NTs/Dox/siRNA nanocarrier were observed when stored in phosphate buffered saline for 7 days, indicating outstanding stability. Moreover, both the cellular uptake efficiency and tumor accumulation effects of NTs on MDA-MB-231 breast cancer cells were significantly improved after modification with tLyp-1. The relative viability of MDA-MB-231 cells was decreased by 70.1% *in vitro* after treatment with tLyp-1/NTs/Dox/siRNA (5 μg/mL Dox). Finally, a synergistic anticancer effect of Dox and siRNA co-loaded in tLyp-1/NTs was achieved in the anticancer treatment of MDA-MB-231 tumor-bearing mice. These findings indicate that food-sourced protein α-lac nanocarriers could be used for the co-delivery of bioactive molecules and RNA, achieving synergistic and efficient therapeutic effects.

1. Introduction

Nanocarriers, as delivery systems for bioactive ingredients in functional foods or drugs for special medical purpose, have attracted a great deal of attention[1]. Yet, several challenges in designing nanocarriers, such as source renewability, sustainability, biocompatibility, or a combination of these properties, remain to be solved. Nanocarriers formed by materials derived from food components, like proteins, offer advantages such as low cost, high biocompatibility, and biodegradability[2]. For example, Shen et al.[1] used biodegradable milk protein β-lactoglobulin amyloid fibrils as efficient nanocarriers for iron fortification. Biocompatible nanocarriers with various morphologies, including nanotubes and nanospheres, and size distributions were fabricated from the edible protein α-lactalbumin (α-lac)[3-5]. Nanotubes (NTs) and nanospheres were designed as delivery systems for hydrophobic bioactive ingredients for use in functional foods[6-8]. Furthermore, it was demonstrated that α-lac NTs with shorter lengths are more favorable for absorption than long NTs and nanospheres[4,9]. However, food-derived protein delivery systems still required further modifications for targeted deliver to specific cells or tissues for pharmaceutical applications.

* Corresponding authors.
E-mail address: binliu@cau.edu.cn (B. Liu); xingli1104@outlook.com (X. Li)
Peer review under responsibility of KeAi Communications Co., Ltd.

10.1016/j.jfutfo.2023.11.002

Cancer is responsible for the majority of mortality worldwide, with an estimation of 17 million cancer death in 2030[10]. Currently, chemotherapy, radiotherapy, and surgery are generally the most efficient treatment strategies[11]. Due to the invasiveness of radiotherapy and surgical procedures, the application of anti-tumor agents remains the most crucial choice for cancer treatment. Doxorubicin (Dox) is commonly used as a chemotherapy agent to treat metastatic cancer[12]. However, the cardiotoxicity and drug resistance of Dox limit its clinical applications[13]. Recently, small interfering RNA (siRNA) was used in combination with Dox to interfere in multiple tumor signaling pathways and silence the gene expression of key signaling molecules[14]. The combination of Dox with siRNA could overcome multidrug resistance by synergistic effects. This combination strategy could treat cancer via different molecular mechanisms, thereby enhancing anti-tumor efficiency[12,15]. Nevertheless, off-target effects remain a great challenge and must be addressed through appropriate design, synthesis, and optimization of the delivery systems[16-17]. Overall, the drawbacks of low delivery efficiency, off-targeting, and severe side effects restrict the clinical application of these delivery systems[18-19]. Therefore, there is an urgent necessity to find more biocompatible biomaterials as cancer drug delivery systems. Additionally, a non-synthetic route for designing nanocarriers from natural sources is required for application in the food and pharmaceutical sectors.

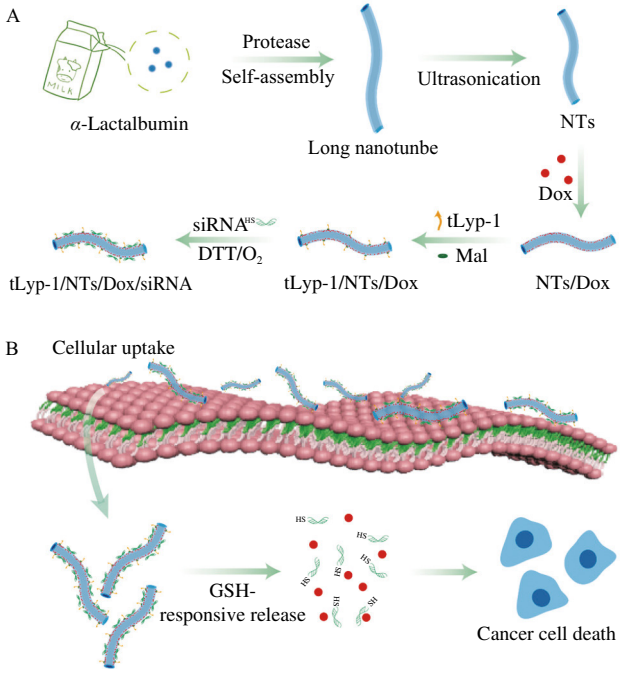

Fig. 1 Schematic illustration of the tumor targeted tLyp-1/NTs/Dox/siRNA nanocarrier. (A) α-Lac peptides self-assembled into NTs after partially hydrolyzed by BLP, Dox loaded into the hydrophobic core of NTs (NTs/Dox) via hydrophobic interactions. NTs/Dox were modified by tLyp-1 through covalent bonds (tLyp-1/NTs/Dox). The disulfide bonds on the surface of NTs were cleaved by DTT and new disulfide bonds were formed between NTs and sulfhydryl-siRNA (tLyp-1/NTs/Dox/siRNA). (B) In cytosol, the disulfide bonds of tLyp-1/NTs/Dox/siRNA were reduced and cleaved by the intracellular GSH, and the Dox and siRNA were released subsequently.

Herein, a nanocarrier of NTs formed by food-sourced α-lac was developed for the co-delivery of Dox and siRNA (Fig. 1). Firstly, NTs were self-assembled from α-lac peptides that hydrolyzed by *Bacillus licheniformis* protease (BLP)[20]. Dox was encapsulated into the hydrophobic inner cores of NTs during the self-assembly process through hydrophobic interactions (NTs/Dox). Then, the tumor-targeted peptide tLyp-1 was covalently grafted onto the surface of NTs (tLyp-1/NTs/Dox). Finally, the disulfide bonds on the surface of NTs could be reduced by *DL*-dithiothreitol (DTT), and sulfhydryl-siRNA was loaded by forming new disulfide bonds with the endogenous cysteines on the surface of NTs through oxidation (tLyp-1/NTs/Dox/siRNA). When tLyp-1/NTs/Dox/siRNA nanocarriers were taken up by tumor cells, siRNA was responsively released under the reduction of high intracellular glutathione (GSH) concentration, which could silence key genes and inhibit the expression of survivin proteins. In the meantime, Dox was released from the nanocarrier and exerted an anti-tumor effect. *In vitro*, the release behavior of Dox and siRNA from tLyp-1/NTs/Dox/siRNA, as well as the cytotoxicity and cellular uptake of tLyp-1/NTs/Dox/siRNA, was studied. Furthermore, the biodistribution of tLyp-1/NTs/Dox/siRNA was investigated *in vivo*. Finally, the anti-tumor efficiency of tLyp-1/NTs/Dox/siRNA was explored in MDA-MB-231 tumor-bearing mice.

2. Materials and methods

2.1 Materials

α-Lac (≥ 85%), Dox (99.5%), *N*-(2-aminoethyl) maleimide (Mal), 1-ethyl-3-(3-dimethylaminoproyl) carbodiimide (EDC), reduced GSH, and DTT were purchased from Sigma Aldrich (St. Louis, MO, USA). The fluorescent hydrophobic dyes Cy3, Cy5, and Cy7-SE were obtained from Fanbo Biochemical Co. (Beijing, China). tLyp-1 peptide was synthesized by GL Biochem. Ltd. (Shanghai, China). siRNA was synthesized by RiboBio Co., Ltd. (Guangzhou, China). The sequences of siRNA were listed in Table S1. BLP was a kind gift from Novozymes, Denmark.

2.2 Preparation of tLyp-1/NTs/Dox/siRNA nanocarriers

NTs with different length distributions were prepared according to the methods reported previously[4]. Briefly, long NTs were self-assembled from the hydrolysis of α-lac (30 mg/mL) by BLP and incubated with calcium ion at 50 °C for 1 h. The short NTs used in this study was obtained by sonicating the long NTs in an ice-water bath[3]. For the preparation of Dox loaded NTs (NTs/Dox), 0.1 mg/mL Dox was mixed with NTs at a volume ratio of 2:1, followed by rotation at 200 r/min for 12 h. To graft the tumor-targeted peptide tLyp-1 onto the surface of NTs/Dox, 0.25 mg of EDC and Mal were added to 1 mL of NTs/Dox solution (1 mg/mL) in sequence at 15 min intervals. The excess EDC and Mal were dialyzed using a dialysis bag (3 500 Da MWCO). Then, 0.82 mg of tLyp-1 peptide was added and reacted for 2 h under gentle stirring, and the product of tLyp-1/NTs/Dox was collected after dialysis for 2 h. Finally, 0.001 mmol/L DTT was incubated with tLyp-1/NTs/Dox at room temperature for 4 h to break the disulfide bonds on NTs. After proper dialysis, tLyp-1/NTs/Dox were cross-linked with siRNA (1:20, *m*/*m*) through the formation of disulfide bonds between NTs and siRNA via oxidation. Finally, nanocarriers of tLyp-1/NTs/Dox/siRNA were obtained by lyophilization and stored at 4 °C for further use.

2.3 Characterization of tLyp-1/NTs/Dox/siRNA nanocarriers

The micromorphology of the nanocarriers was observed by transmission electron microscopy (TEM; JEM-1400, JEOL) after being negatively stained by 3% uranium acetate. Size distribution and zeta potential of the nanocarriers were determined using a dynamic light scattering instrument (Nano-ZS, Malvern Instruments Ltd., Malvern, UK) at 25 °C for a continuous time from 1 to 7 days.

2.4 Loading efficiency of Dox and siRNA in nanocarrier

The loading efficiency (%) of Dox was determined by using UV spectrophotometer (Shimadzu UV-2450, Kyoto, Japan). Specifically, 1 mg tLyp-1/NTs/Dox/siRNA was dissolved in 0.1 mL methyl alcohol. The Dox concentration (mg/mL) could be obtained by the standard curve pre-prepared ($Y = 6.145\ 6X - 0.016\ 7$, $R^2 = 0.993\ 8$), and loading efficiency was calculated as follows:

$$\text{Loading efficiency (\%)} = \frac{m_1}{m_2 - m_1} \quad (1)$$

Where m_1 and m_2 are the weights (mg) of Dox and tLyp/NTs/Dox/siRNA, respectively.

The grafting rate of siRNA on NTs was determined using agarose gel electrophoresis. Briefly, NTs/siRNA were prepared at different weight ratios of NTs to siRNA (20:1, 15:1, 10:1, 5:1, and 0:1). The un-grafted siRNA was detected by electrophoresis using 1% (*m*/*V*) agarose gel.

2.5 Release profile of Dox and siRNA in vitro

tLyp-1/NTs/Dox/siRNA (5 mg) were dissolved in 5 mL phosphate buffered saline (PBS, pH 7.4) containing 10 mmol/L reduced GSH and 0.5% Tween 80 (*V*/*m*). The mixture was then dialyzed using 3 500 Da MWCO dialysis bag in 20 mL PBS. A 1 mL sample was extracted at different time points (0, 3, 6, 9, 12, 18, 24, 30, 36, 42, 48 h), and 1 mL of fresh PBS was added at the same time. The absorbance of the samples was measured using a UV spectrophotometer at 480 nm, as described above.

The release of siRNA was monitored by agarose gel electrophoresis. tLyp-1/NTs/Dox/siRNA at a 20:1 weight ratio of NTs to siRNA were prepared, and other paralleled nanotubes were dealt with 10 mmol/L GSH or 10 mmol/L DTT for 24 h.

2.6 Cytotoxicity analysis for tLyp-1/NTs/Dox/siRNA nanocarriers

MDA-MB-231 cells were purchased from the Cell Resource Center (Peking Union Medical College headquarters of National Infrastructure of Cell Line Resource, NSTT) and were cultured in Dulbecco's Modified Eagle's Medium (DMEM) containing 10% fetal calf serum and 1% penicillin/streptomycin, incubated at 37 °C in a humidified atmosphere of 5% CO_2.

The cytotoxicity of NTs, tLyp-1, free Dox, and siRNA, as well as NTs nanocarriers containing NTs/Dox, NTs/siRNA, NTs/Dox/siRNA, and tLyp-1/NTs/Dox/siRNA were evaluated using a CCK-8 assay. Specifically, 5 000 cells were seeded in 96-well plates and incubated overnight. Then, different samples with an equivalent Dox concentration ranging from 0 to 5 μg/mL were added and cultured for 24 h. In addition, the relative viability of cells was determined by CCK-8 assay, and cells treated with PBS were served as 100% viability. Furthermore, a live/dead cell viability assay (Invitrogen) was used to evaluate the cytotoxicity of different nanocarriers at an equivalent Dox concentration of 5 μg/mL after treating cells for 4 h. The cells were stained with a mixture of 2 μmol/L calcein AM and 4 μmol/L EthD-1 for 20 min, and then observed by confocal laser scanning microscopy (CLSM; A1, Nikon).

2.7 In vitro cellular uptake analysis of nanocarriers

Cellular uptake of NTs and tLyp-1/NTs was determined as described previously with minor modifications[21]. In brief, MDA-MB-231 cells were seeded in confocal Glass Bottom Dishes (Thermo Scientific) at a density of 1×10^5 cells/dish. The preparation of Cy3-loaded NTs was consistent with the loading methods of Dox described above. After removing the free dye, NTs/Cy3 and tLyp-1/NTs/Cy3 were incubated with cells for 4 h. Cells were fixed with 4% paraformaldehyde for 15 min after being rinsed with PBS. Then, the cell nucleus was stained with Hoechst 33342 for 10 min before being observed by CLSM. The cellular uptake of NTs and tLyp-1/NTs was further quantitatively evaluated by flow cytometry. MDA-MB-231 cells were seeded in 6-well plates at a density of 2.5×10^5 cells/well. NTs/Cy5 or tLyp-1/NTs/Cy5 were incubated with the cells for 4 h. Then, the cells were collected and detected by flow cytometry (FC500, Beckman), and the Cy5 fluorescent signals were analyzed under the APC channel.

To study the co-delivery behavior of Dox and siRNA, Dox was replaced by Cy3, and siRNA was decorated with Cy5 (siRNA-Cy5). Then, MDA-MB-231 cells were treated with NTs/Cy3/siRNA-Cy5 and tLyp1/NTs/Cy3/siRNA-Cy5 at a concentration of 100 μg/mL for 4 h. Cells were observed by CLSM with the excitation wavelength at 370, 561, and 654 nm for Hoechst 33342, Cy3, and Cy5, respectively.

2.8 Animals studies

Female BALB/c nude mice (4 weeks) were purchased from Vital River Laboratories (Beijing, China). The mice were housed with a 12 h light/dark cycle at a temperature of (23 ± 2) °C. 1×10^7 MDA-MB-231 cells were injected into the left armpit to establish the tumor mouse model. Mice with tumors grew for 3 weeks and tumor volume reached approximately 150 mm^3 before further evaluations. Tumor diameters were measured using a digital vernier caliper, and volumes were calculated as follows[22]:

$$V = \frac{L \times W^2}{2} \quad (2)$$

Where L and W represent the longest and shortest diameters (mm) of tumors, respectively.

All animal experiments were performed following the Guide for the Care and Use of Laboratory Animals and were approved by the Experimental Animal Ethics Committee in Beijing.

2.8.1 Biodistribution of NTs and tLyp-1/NTs in vivo

NTs/Cy7 and tLyp-1/NTs/Cy7 were injected into tumor-bearing mice established as mentioned above via the tail vein. Fluorescence

images of the mice were acquired by an *in vivo* imaging system (FXPro, Kodak) at 1, 2, 4, and 8 h post-injection. Then, the mice were sacrificed at 8 h, tumors and major organs (heart, liver, spleen, lung, and kidney) were collected. The fluorescence images of tumors and organs were captured by the imaging system (FXPro, Kodak).

2.8.2 Changes of survivin protein levels in tumors

Changes in the relative survivin protein expression levels in tumor tissues were characterized after treatment with different nanocarriers. Tumor tissue was collected, and part of the tumor was ground. Total protein from the tumor tissue was lysed by RIPA lysis buffer, and survivin protein expression levels was analyzed by Western blot[23]. In detail, the proteins were separated and transferred to polyvinylidene difluoride (PVDF) membranes. After being blocked by 5% (*m*/*V*) skimmed milk for 2 h, the PVDF membranes were incubated with a survivin antibody (1:600, Servicebio, Wuhan, China) at 4 °C overnight. After being washed twice with Tris-buffered saline with 0.1% Tween (TBST), the PVDF membranes were incubated with a horseradish peroxidase-conjugated secondary antibody (1:10 000, Invitrogen) for 2 h. Then, protein expression was detected with an ECL detection reagent (Dingguo Changsheng, Beijing, China) after the PVDF membranes were washed. *β*-Actin (Servicebio, Wuhan, China) was used as internal control.

2.8.3 Anti-tumor efficiency of tLyp-1/NTs/Dox/siRNA nanocarriers in vivo

The tumor-bearing mice were randomly divided into six groups (n = 8). Different formulations, including PBS, Dox, siRNA, Dox/siRNA, NTs/Dox/siRNA and tLyp-1/NTs/Dox/siRNA, were intravenously injected every other day at an equivalent Dox concentration of 5 mg/kg body weight. Body weights and tumor volumes were monitored and recorded. Mice were sacrificed after 14 days of treatment, and tumors and major organs (heart, liver, spleen, lung, and kidney) were collected and fixed in 4% formaldehyde solution.

The tumors were dehydrated and embedded in paraffin blocks for immunohistochemical analysis. Hematoxylin and eosin (HE), terminal deoxynucleotidyl transferase dUTP nick end labelling (TUNEL), and Ki-67 staining were used to observe the anti-tumor effect of nanocarriers. The major organs (heart, liver, spleen, lung, and kidney) were stained with HE to assess the toxicity of nanocarriers.

2.9 Statistical analysis

Statistical data evaluations were performed using Graph-Pad Prism 9.0.0 (Graphpad, San Diego, CA, USA). Data are expressed as mean ± standard deviation (SD) unless stated otherwise. Cell viability, tumor weight, and survivin protein expression were analyzed using one-way repeated measures ANOVA (n = 8). Tumor volume and Dox release were analyzed using two-way ANOVA, followed by Bonferroni post-hoc test. P-values less than 0.05 were considered statistically significant.

3. Results and discussion

3.1 Characterization of Dox and siRNA-loaded nanotubes

The micromorphology of NTs nanocarriers is shown in Fig. 2A. The tubular micro-structures of the nanocarriers remained unchanged in the presence or absence of Dox and siRNA. While the length of NTs showed negligible changes, the thickness of tLyp-1/NTs/Dox/siRNA was higher than that of pure NTs, as observed in TEM images. This might be due to the loading of Dox and siRNA, as well as the conjugating of tLyp-1 peptides, which increased the thickness of NTs. In addition, due to the grafting of siRNA, the surface charge of NTs was reversed from –24.4 to 3.4 mV (Fig. 2B), leading to

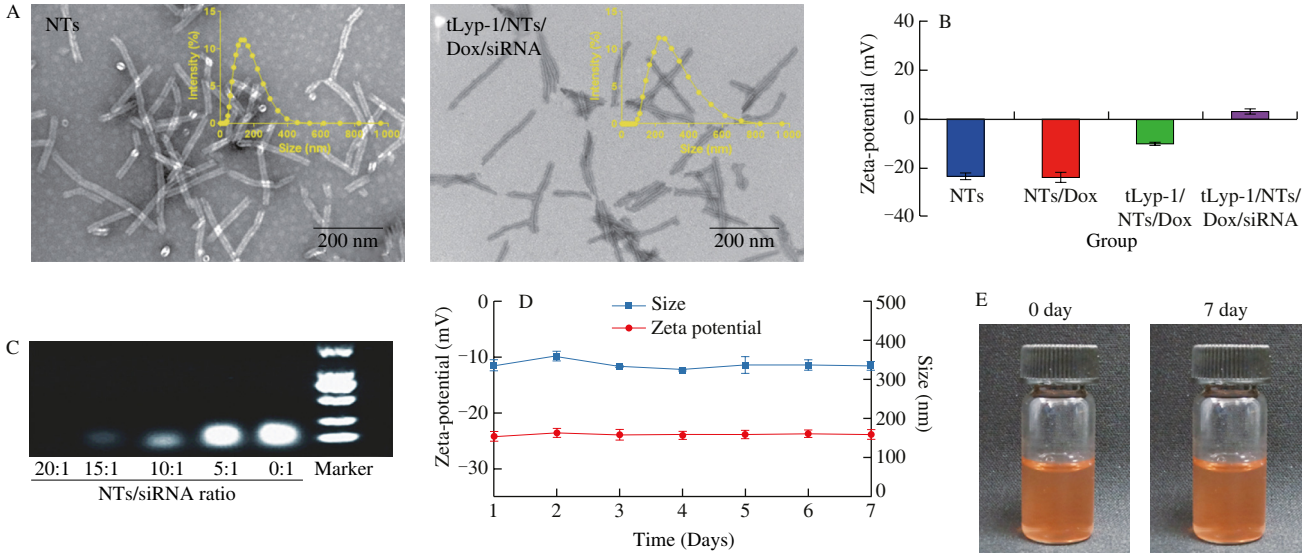

Fig. 2 Characterizations of NTs nanocarriers before and after the loading of Dox and siRNA. (A) The micromorphology of NTs and tLyp-1/NTs/Dox/siRNA observed by TEM. (B) Zeta-potential changes of various nanocarriers during the preparation processes of tLyp-1/NTs/Dox/siRNA. Data represent mean ± SD (n = 3). (C) Agarose gel electrophoresis for NTs/siRNA with the weight ratio of 20:1, 15:1, 10:1, 5:1, and 0:1 (NTs:siRNA). Naked siRNA was used as control. (D) The storage stability of size and Zeta-potential of tLyp-1/NTs/Dox/siRNA in PBS over 7 days. Data represent mean ± SD (n = 3). (E) The image of tLyp-1/NTs/Dox/siRNA that was stored for 7 days in PBS.

the aggregation of NTs and an increase in thickness. Similar results were observed in a previous work, which demonstrated that the size distribution increased due to the bridging agglomeration of hydroxyapatite/polyethyleneimine (PEI) nanorods and nucleic acids[24]. There was no significant change in the loading efficiency of Dox after the grafting of siRNA (tLyp-1/NTs/Dox: 5.05%, tLyp-1/NTs/Dox/siRNA: 4.92%; Table S2). The optimal charge ratio was evaluated using a gel retardation assay[25]. Fig. 2C showed that the optimal complexation ratio for NTs to siRNA was 20:1 (*m*/*m*). Furthermore, the size and zeta potential of tLyp-1/NTs/Dox/siRNA exhibited negligible changes when stored for 7 days in PBS (Fig. 2D). The improved stability of tLyp-1/NTs/Dox/siRNA might be attributed to the recross-linking of endogenous disulfide bonds on the surface of NTs and siRNA[26]. Additionally, no color changes and precipitation occurred after 7 days of storage, indicating outstanding stability of tLyp-1/NTs/Dox/siRNA, which paves the way for its further application *in vivo* (Fig. 2E).

3.2 GSH-responsive release of Dox and siRNA from nanocarriers

It has been reported that the concentration of GSH in cancer cells is much higher than that in normal cells[27]. To mimic the higher GSH concentration in tumor cells, 10 mmol/L GSH was added to PBS (pH 7.4) before the release experiment of Dox was conducted. As shown in Fig. 3A, the structure of tLyp-1/NTs/Dox/siRNA was disrupted by the addition of GSH, resulting in the corresponding release of Dox and siRNA. This disruption occurred due to the reductive activity of GSH, which can cleave the cross-linked disulfide bonds between siRNA and NTs in tLyp-1/NTs/Dox/siRNA[28]. The maximum release of Dox reached 81.07% at 42 h in the presence of GSH, while only 40.86% of Dox was released without GSH (Fig. 3B). The release of siRNA was qualitatively determined by agarose gel electrophoresis. When the weight ratio of NTs to siRNA was 20:1, the corresponding band disappeared. However, the band appeared with the addition of 10 mmol/L GSH or DTT (Fig. 3C). Due to the stronger reductive activity of DTT compared to GSH, the siRNA band after adding DTT was brighter than after adding GSH[29]. These results indicated that the release of siRNA and Dox exhibites GSH-responsive behavior, which was favorable for their responsive release in cancer cells.

3.3 The uptake of NTs and tLyp-1/NTs by breast cancer cells

The cellular uptake results of NTs and tLyp-1/NTs by human breast cancer cell MDA-MB-231 are shown in Fig. 4. Obviously, cells incubated with tLyp-1/NTs showed significantly more red fluorescence signals in the cytoplasm than those treated with NTs (Fig. 4A), suggesting that tLyp-1/NTs can effectively target tumor cells. Flow cytometry results also confirmed that the tumor-targeted peptide (tLyp-1) could improve the uptake of NTs in MDA-MB-231 cells (Fig. 4B). The cellular uptake efficiency of tLyp-1/NTs/Cy5 was higher than that of NTs/Cy5, probably due to the specific recognition between tLyp-1 peptide and neuropilin 1 (NRP1) receptors on the MDA-MB-231 cell membranes[30]. These results indicated that the tLyp-1/NTs nanocarrier had great potential for targeted drug delivery in anti-cancer therapy.

3.4 Cytotoxicity of NTs nanocarriers in MDA-MB-231 cells

The anti-cancer effect of nanocarriers at the cellular level was evaluated by incubating tLyp-1/NTs/Dox/siRNA with MDA-MB-231 cells for 24 h. Firstly, cytotoxicity was quantified via a CCK-8 assay. As shown in Fig. 5A, no significant cytotoxicity was observed in NTs and NTs/siRNA, even at the highest concentration (equivalent to 5 μg/mL Dox). However, Dox exhibited certain cytotoxicity to cancer cells. Interestingly, when Dox and siRNA were co-loaded into tLyp-1/NTs, a synergistic anti-cancer effect was observed in tLyp-1/NTs/Dox/siRNA. Specifically, the cell viability of the tLyp-1/NTs/Dox/siRNA treatment group decreased significantly to 29.9% compared to the free Dox and siRNA treatment group (49.77% and 98.54%, respectively) (Fig. S1). Hydrophobic Dox delivered without nanocarrier had a low absorption rate, resulting in a limited anticancer effect. Additionally, siRNA may be degraded rapidly without the protection of a nanocarrier[31-32]. Herein, the co-loading of the two via tLyp-1/NTs nanocarrier was proven to have the ability to protect and enhance the anticancer efficacy of Dox and siRNA. Furthermore, the anticancer efficacy was further investigated by a live-dead assay. As shown in Fig. 5B, the area of dead cells (red) in the tLyp-1/NTs/Dox/siRNA treatment group was obviously larger than that in the other groups, especially in the NTs/Dox and NTs/siRNA group, indicating that a

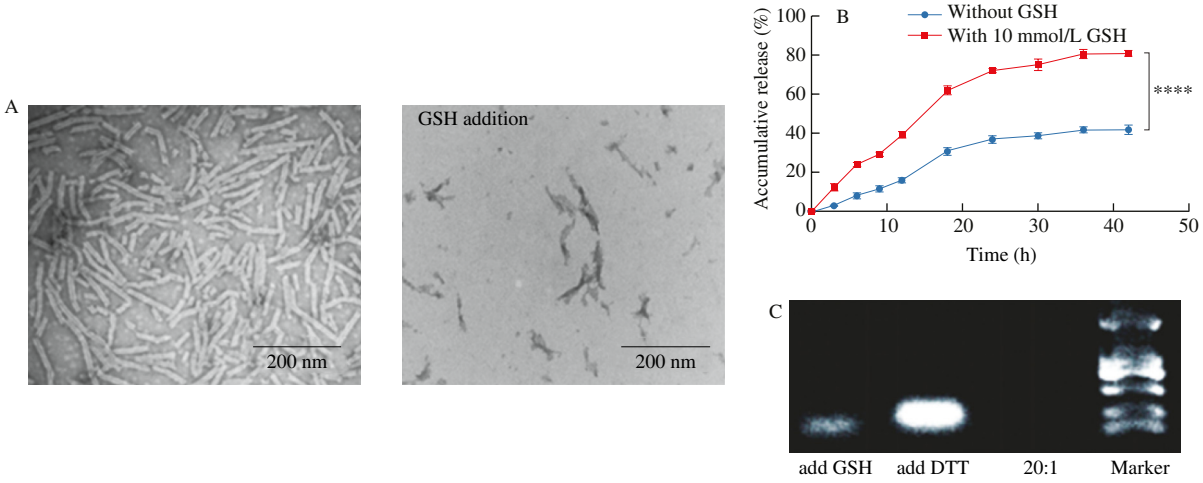

Fig. 3 GSH-responsive release profile of tLyp-1/NTs/Dox/siRNA nanocarrier. (A) TEM images of tLyp-1/NTs/Dox/siRNA before and after the addition of 10 mmol/L GSH. (B) The accumulative release of Dox from tLyp-1/NTs/Dox/siRNA triggered by GSH *in vitro*. Data represent mean ± SD (n = 3). ****P < 0.000 1. (C) Agarose gel electrophoresis of siRNA released from tLyp-1/NTs/Dox/siRNA triggered by 10 mmol/L GSH or DTT.

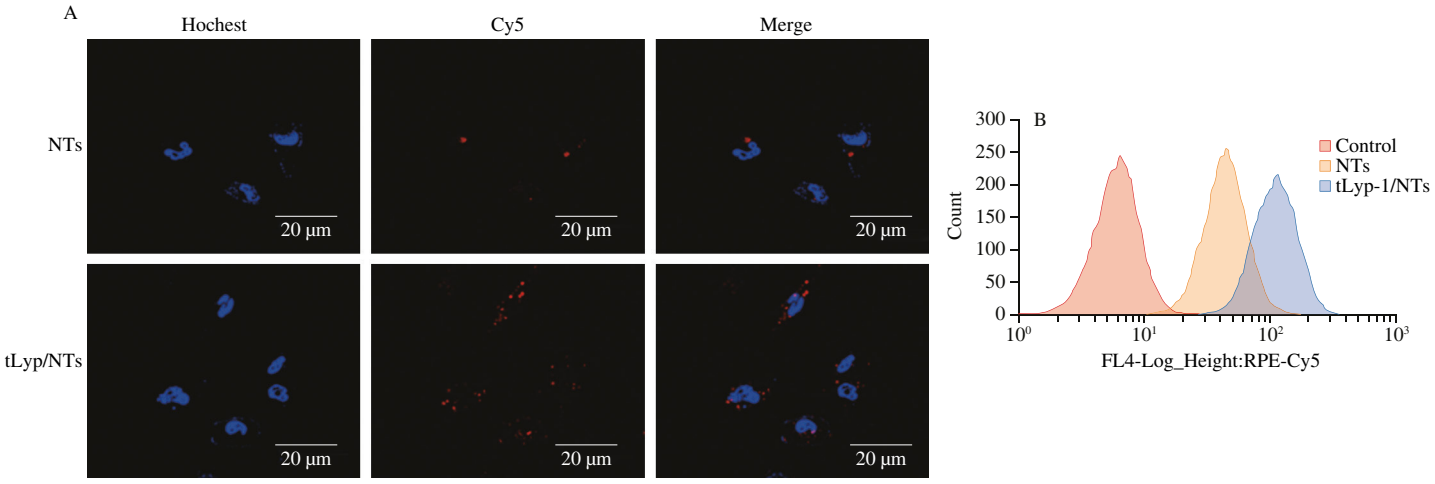

Fig. 4 Cellular uptake of tLyp-1/NTs and NTs in MDA-MB-231 cells. (A) CLSM images of cellular uptake of tLyp-1/NTs/Cy5 and NTs/Cy5 in MDA-MB-231 cells after incubating for 4 h. The nuclei and nanocarriers were labeled by Hoechst 33342 (blue) and Cy5 (red), respectively. (B) Flow cytometry for MDA-MB-231 cells incubated with tLyp-1/NTs/Cy5 or NTs/Cy5 for 4 h.

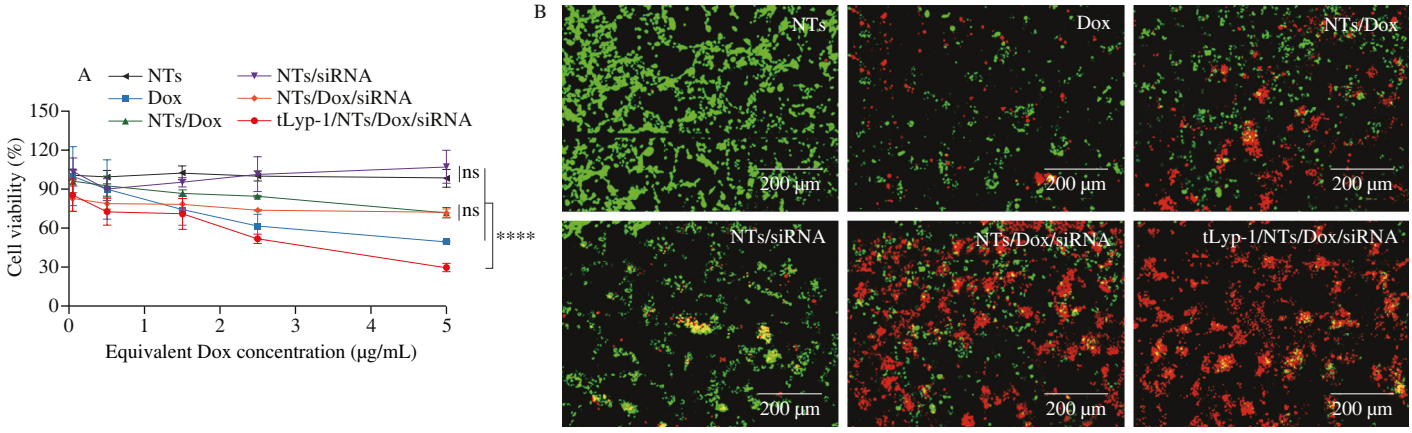

Fig. 5 The cytotoxicity of various formulations to MDA-MB-231 cells. (A) Cell viability of MDA-MB-231 cells incubated with various formulations (NTs, free Dox, NTs/Dox, NTs/siRNA, NTs/Dox/siRNA, and tLyp-1/NTs/Dox/siRNA) at different concentrations. ****$P < 0.000\ 1$. Data represent mean ± SD ($n = 6$). (B) Live/dead analysis of MDA-MB-231 cells after treated by different formulations at an equivalent Dox concentration of 5 μg/mL for 4 h. Live cells were green; Dead cells were red.

synergistic anti-tumor effect was achieved when co-loading Dox and siRNA in tLyp-1/NTs. Overall, these results demonstrate that tLyp-1/NTs/Dox/siRNA can improve the anticancer efficiency of Dox and siRNA, achieving a synergistic anti-tumor effect simultaneously.

3.5 *Biodistribution of NTs and tLyp-1/NTs in vivo*

The biodistributions of Cy7-labeled NTs and tLyp-1/NTs in MDA-MB-231 cell xenografted mice models were investigated. As shown in Fig. 6A, the accumulation of NTs/Cy7 and tLyp-1/NTs/Cy7 at the tumor site was acquired at 1, 2, 4, and 8 h after intravenous injection. The fluorescent signal of tLyp-1/NTs/Cy7 in the tumor was stronger than that of NTs/Cy7 after 8 h of tail vein injection. This difference in the excised tumor was clearly observed in Fig. 6B, and the fluorescence intensity in the tLyp-1/NTs/Cy7 group was 1.1 times higher than that in the NTs/Cy7 group (Fig. 6C). The obvious distinction between NTs and tLyp-1/NTs in tumor accumulation indicated that tLyp-1 could enhance the targeting ability of NTs to tumors *in vivo*, which was consistent with the cancer cellular uptake results in Fig. 4.

3.6 *Anti-tumor efficacy of tLyp-1/NTs/Dox/siRNA in vivo*

The anti-cancer efficiency of the tLyp-1/NTs/Dox/siRNA nanocarrier was further evaluated in MDA-MB-231 cell xenografted mouse models. As shown in Figs. 7A and 7B, the PBS group had the fastest tumor growth compared to the other groups. While for free Dox, siRNA, or the combination of them, a slightly suppressed tumor growth was observed, probably duo to the high metabolic rates of Dox and siRNA. Remarkably, the tumor growth of the NTs/Dox/siRNA and tLyp-1/NTs/Dox/siRNA groups was significantly suppressed when loaded into NTs at an equivalent 5 μg/mL Dox concentration. NTs grafted with tLyp-1 showed a better tumor suppressing effect than other samples. Survivin, highly expressed in cancer cells, is the inhibitor of apoptosis protein which could block cell death[33-34]. Here, the siRNA loaded in the nanocarrier was applied to silence and downregulate the expression of survivin protein. Therefore, to elucidate whether the tumor suppression was related to the downregulation of survivin by siRNA, survivin proteins were extracted from tumor tissues after treatment with various formulations, and the expression of survivin protein was further analyzed by

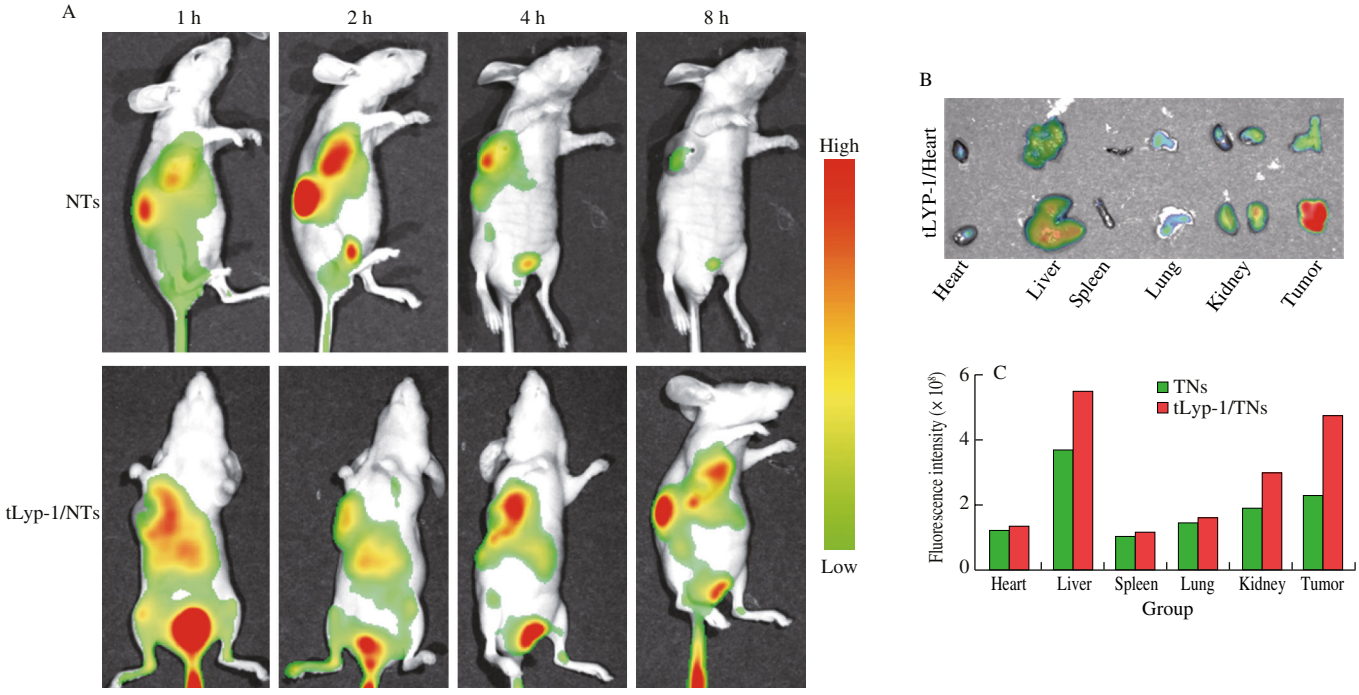

Fig. 6 *In vivo* biodistribution of Cy7-labled NTs and tLyp-1/NTs on MDA-MB-231 tumor-bearing mice model. (A) Representative fluorescence images of NTs/Cy7 and tLyp-1/NTs/Cy7 in tumor xenografted mouse models at 1, 2, 4, and 8 h post-injection. (B) The fluorescent images and (C) fluorescence intensity of Cy7-labeled NTs and tLyp-1/NTs in major organs (heart, liver, spleen, lung, and kidney) and tumors after 8 h tail vein injection.

western blot. As shown in Figs. 7C and 7D, the expression of survivin protein was not decreased in the free Dox, siRNA, and Dox/siRNA treatment groups. However, it was nearly disappeared in the NTs/Dox/siRNA and tLyp-1/NTs/Dox/siRNA groups. The expression of survivin protein decreased by 60.9% and 71.4% for NTs/Dox/siRNA and tLyp-1/NTs/Dox/siRNA, respectively. The possible anti-tumor mechanism of siRNA is that siRNA interfered with the mRNA of survivin protein, thereby blocking the expression of survivin protein and ultimately promoting apoptosis of MDA-MB-231 cancer cells[35].

Moreover, the histological results showed that the nuclei (purple) of the solid tumor cells were reduced after tLyp-1/NTs/Dox/siRNA treatment compared to other formulations (free Dox, siRNA, Dox/siRNA, and NTs/Dox/siRNA), indicating that tLyp-1/NTs/Dox/siRNA had the best anti-tumor effect (Fig. 7E). Most importantly, no side effects were observed in the major organs with tLyp-1/NTs/Dox/siRNA treatment (Fig. S2). The immunofluorescence results also showed the most significant decrease in cell proliferation (blank areas in the Ki-67 group) and apoptotic cell signals (green in the TUNEL group) after Lyp-1/NTs/Dox/siRNA treatment (Fig. 7E). All these results indicated a synergistic anti-tumor effect of Dox and siRNA when they are co-loaded in the tLyp-1/NTs nanocarrier. In general, tLyp-1/NTs/Dox/siRNA could effectively reduce the expression of survivin protein, eventually promoting the apoptosis of cancer cells.

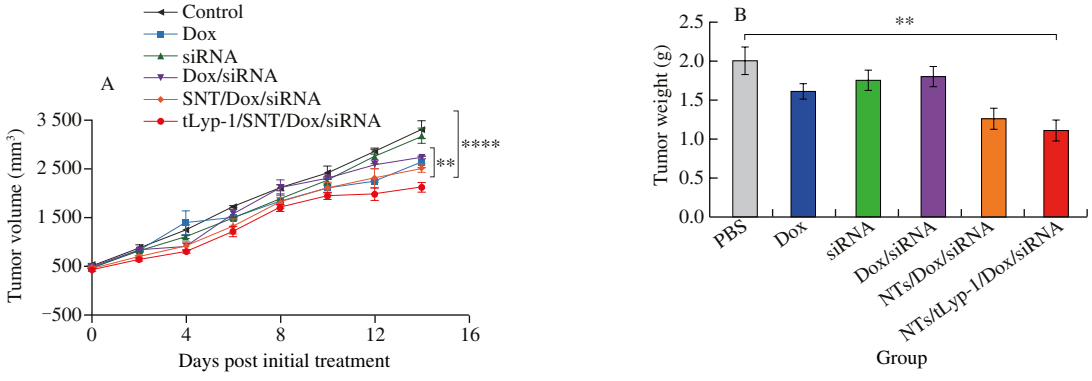

Fig. 7 *In vivo* anti-tumor effects of various nanocarriers on MDA-MB-231 tumor-bearing mice. The volume (A) and weights (B) of tumors in MDA-MB-231 bearing mice after treatment with various formulations (PBS, Dox, siRNA, Dox/siRNA, NTs/Dox/siRNA, and tLyp-1/NTs/Dox/siRNA). (C) The protein levels of survivin in the tumor tissues that were detected by Western blot. (D) Western blot analyses of survivin-protein after treatment with different formulations (PBS, Dox, siRNA, Dox/siRNA, NTs/Dox/siRNA, and tLyp-1/NTs/Dox/siRNA). (E) HE, Ki-67, and TUNEL staining analyses of tumor tissues after treatment with PBS and other formulations (free Dox, siRNA, Dox/siRNA, NTs/Dox/siRNA, and tLyp-1/NTs/Dox/siRNA). Data are expressed as mean ± SD (n = 8), * P < 0.05, ** P < 0.01, **** P < 0.000 1.

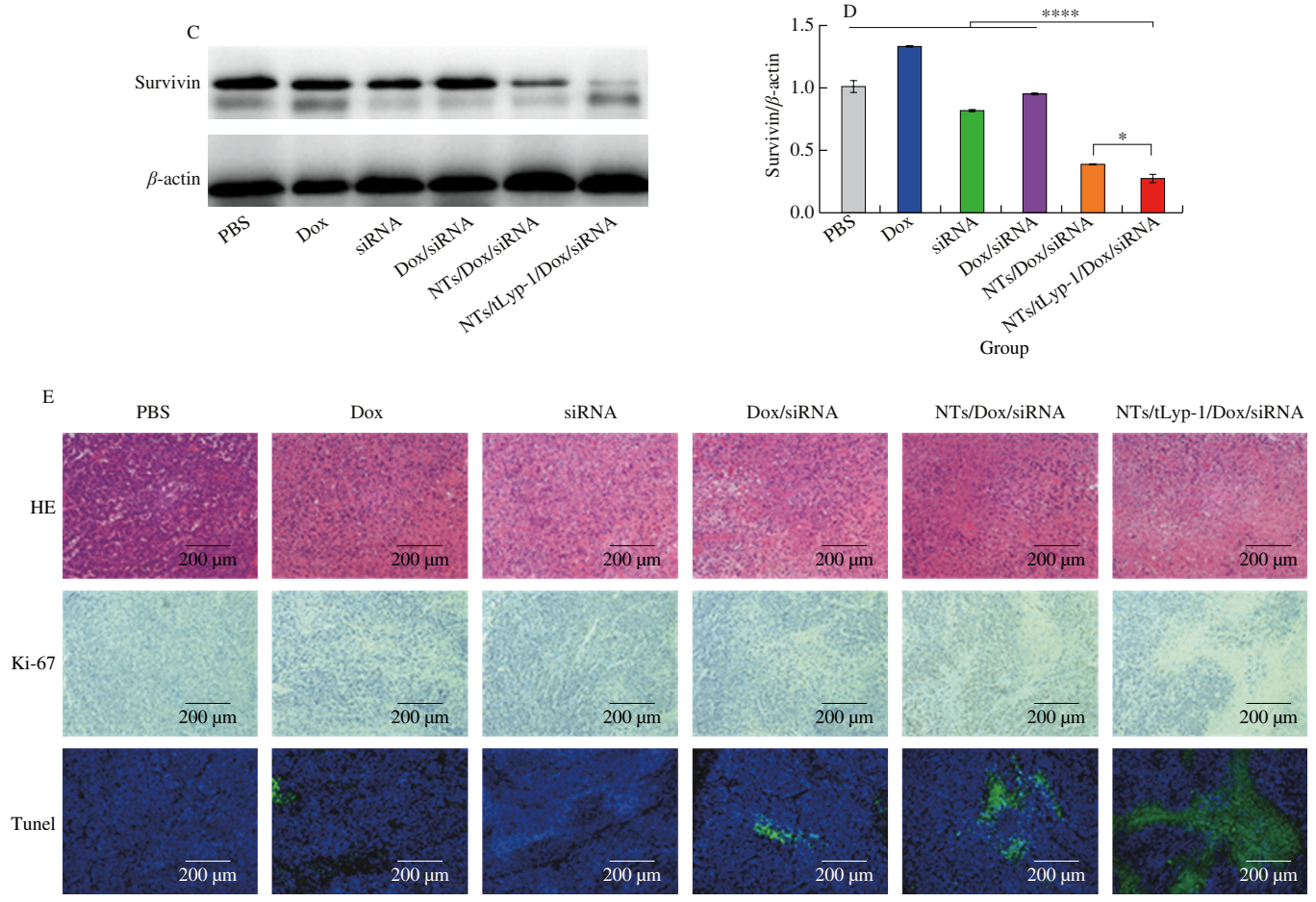

Fig. 7 (*Continued*)

4. Conclusions

In summary, a nanocarrier of food-sourced α-lac NTs was prepared for the codelivery of anti-tumor agents of Dox and siRNA. The incorporation of the tumor-targeting peptide tLyp-1 onto the surface of NTs enables precise delivery of Dox and siRNA to MDA-MB-231 cells. Our findings demonstrated that tLyp-1/NTs/Dox/siRNA nanocarriers are responsive to the tumor microenvironment, specifically the high GSH concentration within the cytoplasm of cancer cells, leading to the subsequent release of loaded Dox and siRNA. tLyp-1/NTs/Dox/siRNA could target and accumulate to the MDA-MB-231 cells that characterized by CLSM and flow cytometry *in vitro*. Finally, it was confirmed that tLyp-1/NTs/Dox/siRNA had the ability to synergistically enhance the anti-tumor effect of Dox and siRNA when applied in the MDA-MB-231 cell xenografted mouse model *in vivo*. Moreover, the expression of survivin protein was downregulated via the Western blot analysis. This study suggests the potential of milk protein-derived nanocarriers as effective platforms for the co-deliver bioactive molecules and siRNA, offering promising prospects for combined chemo and gene therapy in the treatment of cancer.

Conflicts of interest

The authors declare that there are no conflicts of interest regarding the publication of this paper.

Acknowledgments

This work is supported by the China National Postdoctoral Program for Innovative Talents (BX2021364), and the China Postdoctoral Science Foundation (2021M703525).

Appendix A. Supplementary data

Supplementary data associated with this article can be found, in the online version, at http://doi.org/10.1016/j.jfutfo.2023.11.002.

Reference

[1] Y. Shen, L. Posavec, S. Bolisetty, et al., Amyloid fibril systems reduce, stabilize and deliver bioavailable nanosized iron, Nat. Nanotechnol. 12 (2017) 642-647. http://doi.org/10.1038/nnano.2017.58.

[2] A.O. Elzoghby, W.M. Samy, N.A. Elgindy, Protein-based nanocarriers as promising drug and gene delivery systems, J. Control Release 161 (2012) 38-49. http://doi.org/10.1016/j.jconrel.2012.04.036.

[3] W. Bao, F. Tian, C. Lyu, et al., Experimental and theoretical explorations of nanocarriers' multistep delivery performance for rational design and anticancer prediction, Sci. Adv. 7 (2021) eaba2458. http://doi.org/10.1126/sciadv.aba2458.

[4] C. Bao, B. Liu, B. Li, et al., Enhanced transport of shape and rigidity-tuned alpha-lactalbumin nanotubes across intestinal mucus and cellular barriers, Nano Lett. 20 (2020) 1352-1361. http://doi.org/10.1021/acs.nanolett.9b04841.

[5] B. Liu, B. Liu, R. Wang, et al., alpha-Lactalbumin self-assembled nanoparticles with various morphologies, stiffnesses, and sizes as pickering

stabilizers for oil-in-water emulsions and delivery of curcumin, J. Agric. Food Chem. 69 (2021) 2485-2492. http://doi.org/10.1021/acs.jafc.0c06263.

[6] R. Chang, B. Liu, Q. Wang, et al., The encapsulation of lycopene with α-lactalbumin nanotubes to enhance their anti-oxidant activity, viscosity and colloidal stability in dairy drink, Food Hydrocoll. 131 (2022) 107792. http://doi.org/10.1016/j.foodhyd.2022.107792.

[7] Q. Wang, W. Yu, Z. Li, et al., The stability and bioavailability of curcumin loaded α-lactalbumin nanocarriers formulated in functional dairy drink, Food Hydrocoll. 131 (2022) 107807. http://doi.org/10.1016/j.foodhyd.2022.107807.

[8] G. Hou, Y. Li, Q. Wang, et al., iRGD-grafted *N*-trimethyl chitosan-coated protein nanotubes enhanced the anticancer efficacy of curcumin and melittin, Int. J. Biol. Macromol. 222 (2022) 348-359. http://doi.org/10.1016/j.ijbiomac.2022.09.171.

[9] Y. Li, W. Li, W. Bao, et al., Bioinspired peptosomes with programmed stimuli-responses for sequential drug release and high-performance anticancer therapy, Nanoscale 9 (2017) 9317-9324. http://doi.org/10.1039/c7nr00598a.

[10] M.J. Thun, J.O. DeLancey, M.M. Center, et al., The global burden of cancer: priorities for prevention, Carcinogenesis 31 (2010) 100-110. http://doi.org/10.1093/carcin/bgp263.

[11] G. Radha, M. Lopus, The spontaneous remission of cancer: current insights and therapeutic significance, Transl Oncol. 14 (2021) 101166. http://doi.org/10.1016/j.tranon.2021.101166.

[12] J. Zhuang, S. Chen, Y. Hu, et al., Tumour-targeted and redox-responsive mesoporous silica nanoparticles for controlled release of doxorubicin and an siRNA against metastatic breast cancer, Int. J. Nanomed. 16 (2021) 1961-1976. http://doi.org/10.2147/IJN.S278724.

[13] C. Liu, C. Tang, C. Yin, Co-delivery of doxorubicin and siRNA by all-trans retinoic acid conjugated chitosan-based nanocarriers for multiple synergistic antitumor efficacy, Carbohydr. Polym. 283 (2022) 119097. http://doi.org/10.1016/j.carbpol.2022.119097.

[14] C.M. Hu, S. Aryal, L. Zhang, Nanoparticle-assisted combination therapies for effective cancer treatment, Ther. Deliv. 1 (2010) 323-334. http://doi.org/10.4155/tde.10.13.

[15] Y. Li, X. Li, Y. Lu, et al., Co-delivery of *Poria cocos* extract and doxorubicin as an 'all-in-one' nanocarrier to combat breast cancer multidrug resistance during chemotherapy, Nanomedicine 23 (2020) 102095. http://doi.org/10.1016/j.nano.2019.102095.

[16] K. Kumar, B. Maiti, P. Kondaiah, et al., Efficacious gene silencing in serum and significant apoptotic activity induction by survivin downregulation mediated by new cationic gemini tocopheryl lipids, Mol. Pharm. 12 (2015) 351-361. http://doi.org/10.1021/mp500620e.

[17] A.L. Jackson, P.S. Linsley, Recognizing and avoiding siRNA off-target effects for target identification and therapeutic application, Nat. Rev. Drug Discov. 9 (2010) 57-67. http://doi.org/10.1038/nrd3010.

[18] S. Bano, F. Ahmed, F. Khan, et al., Enhancement of the cancer inhibitory effect of the bioactive food component resveratrol by nanoparticle based delivery, Food Funct. 11 (2020) 3213-3226. http://doi.org/10.1039/c9fo02445j.

[19] K. Yang, Z. Yang, G. Yu, et al., Polyprodrug nanomedicines: an emerging paradigm for cancer therapy, Adv. Mater. 34 (2022) e2107434. http://doi.org/10.1002/adma.202107434.

[20] J. Zhang, Q. Wang, B. Liu, et al., The kinetic mechanism of cations induced protein nanotubes self-assembly and their application as delivery system, Biomaterials 286 (2022) 121600. http://doi.org/10.1016/j.biomaterials.2022.121600.

[21] X.D. Wang, Y.L. Mao, C.S. Sun, et al., A versatile gas-generator promoting drug release and oxygen replenishment for amplifying photodynamic-chemotherapy synergetic anti-tumor effects, Biomaterials 276 (2021) 120985. http://doi.org/ARTN 120985.

[22] A. Tabriz, M.A.U.R. Alvi, M.B.K. Niazi, et al., Quaternized trimethyl functionalized chitosan based antifungal membranes for drinking water treatment, Carbohyd. Polym. 207 (2019) 17-25. http://doi.org/10.1016/j.carbpol.2018.11.066.

[23] S. Yang, D. Wang, X. Zhang, et al., cRGD peptide-conjugated polyethylenimine-based lipid nanoparticle for intracellular delivery of siRNA in hepatocarcinoma therapy, Drug Deliv. 28 (2021) 995-1006. http://doi.org/10.1080/10717544.2021.1928794.

[24] J. Klesing, S. Chernousova, M. Epple, Freeze-dried cationic calcium phosphatenanorods as versatile carriers of nucleic acids (DNA, siRNA), J. Mater. Chem. 22 (2012) 199-204. http://doi.org/10.1039/c1jm13502c.

[25] O. Aydin, D. Kanarya, U. Yilmaz, et al., Determination of optimum ratio of cationic polymers and small interfering rna with agarose gel retardation assay, Methods Mol. Biol. 2434 (2022) 117-128. http://doi.org/10.1007/978-1-0716-2010-6_7.

[26] H.I. Chiu, A.D. Ayub, S.N.A. Mat Yusuf, et al., Docetaxel-loaded disulfide cross-linked nanoparticles derived from thiolated sodium alginate for colon cancer drug delivery, Pharmaceutics 12 (2020) 38. http://doi.org/10.3390/pharmaceutics12010038.

[27] N. Yan, L. Lin, C. Xu, et al., A GSH-gated DNA nanodevice for tumor-specific signal amplification of microRNA and MR imaging-guided theranostics, Small 15 (2019) e1903016. http://doi.org/10.1002/smll.201903016.

[28] S. Yu, J. Ding, C. He, et al., Disulfide cross-linked polyurethane micelles as a reduction-triggered drug delivery system for cancer therapy, Adv. Healthc. Mater. 3 (2014) 752-760. http://doi.org/10.1002/adhm.201300308.

[29] B. Lei, M. Wang, Z. Jiang, et al., Constructing redox-responsive metal-organic framework nanocarriers for anticancer drug delivery, ACS Appl. Mater. Interfaces. 10 (2018) 16698-16706. http://doi.org/10.1021/acsami.7b19693.

[30] W. Wang, M. Li, Z. Zhang, et al., Design, synthesis and evaluation of multi-functional tLyP-1-hyaluronic acid-paclitaxel conjugate endowed with broad anticancer scope, Carbohydr. Polym. 156 (2017) 97-107. http://doi.org/10.1016/j.carbpol.2016.08.100.

[31] J. Qian, M. Xu, A. Suo, et al., Folate-decorated hydrophilic three-arm star-block terpolymer as a novel nanovehicle for targeted co-delivery of doxorubicin and Bcl-2 siRNA in breast cancer therapy, Acta Biomater. 15 (2015) 102-116. http://doi.org/10.1016/j.actbio.2014.12.018.

[32] M.A. Jackson, T.A. Werfel, E.J. Curvino, et al., Zwitterionic nanocarrier surface chemistry improves siRNA tumor delivery and silencing activity relative to polyethylene glycol, ACS Nano 11 (2017) 5680-5696. http://doi.org/10.1021/acsnano.7b01110.

[33] P. Norouzi, H. Motasadizadeh, F. Atyabi, et al., Combination therapy of breast cancer by codelivery of doxorubicin and survivin siRNA using polyethylenimine modified silk fibroin nanoparticles, ACS Biomater Sci. Eng. 7 (2021) 1074-1087. http://doi.org/10.1021/acsbiomaterials.0c01511

[34] Y. Zhao, T. Zhao, Y. Cao, et al., Temperature-sensitive lipid-coated carbon nanotubes for synergistic photothermal therapy and gene therapy, ACS Nano 15 (2021) 6517-6529. http://doi.org/10.1021/acsnano.0c08790.

[35] M. Lopez-Fraga, T. Martinez, A. Jimenez, RNA interference technologies and therapeutics: from basic research to products, BioDrugs 23 (2009) 305-332. http://doi.org/10.2165/11318190-000000000-00000.